Longwave Radiation on Snow-Covered Mountainous Surfaces

CHRISTIAN PLÜSS AND ATSUMU OHMURA

Institute of Geography, Swiss Federal Institute of Technology, Zurich, Switzerland

(Manuscript received 1 February 1996, in final form 26 December 1996)

ABSTRACT

Longwave radiation in snow-covered alpine environments was investigated based on LOWTRAN7 calculations. The irradiance from the sky and from the surrounding topography were determined separately in order to detect the influence of the topography on longwave radiation balance. Sensitivity studies showed that the irradiance from the surrounding terrain is determined primarily by the atmospheric conditions within the investigated area and by the surface temperature of the surrounding terrain. In snow-covered environments, the air temperature is usually above the snow surface temperature and the effects of the air between the topography and the receiving surface may be relevant.

Longwave irradiance from the surrounding terrain is an important component of the energy balance at the snow surface on inclined slopes and should be considered for areal investigations. A simple parameterization that accounts for the effects of the air is proposed for efficient calculation of longwave irradiance from snow-covered topography.

1. Introduction

In most environments where a seasonal snow cover is present, the radiation balance is the dominant energy source for snowmelt (e.g., Male and Granger 1981; Ohmura 1982; Aguado 1985). Unlike the snow cover in plains, alpine snow fields receive radiation not only from the sky, but also from reflection and emission of the surrounding topography. Hence, in complex alpine topography, the radiation balance at a snow surface may be written as

$$\mathrm{NR} = (I_s + D_s + D_t)(1 - \alpha) + L_s^{\downarrow} + L_t^{\downarrow} - L^{\uparrow}, \quad (1)$$

whereby NR is the net irradiance, I_s is the direct solar irradiance, D_s is the diffuse sky irradiance, D_t is the diffuse irradiance from the surrounding terrain, α is the albedo of the snow cover, $L_s^{\downarrow}$ is the incoming atmospheric longwave irradiance, $L_t^{\downarrow}$ is the longwave irradiance from the surrounding terrain, and $L^{\uparrow}$ is the outgoing longwave irradiance. Exact knowledge of the radiation balance, including the effects of the radiation from the surrounding terrain, is important in many areal applications, for example, in snowmelt runoff modeling, in avalanche forecasting, for energy balance investigations on alpine glaciers, or for the detection of the errors of radiation measurements in complex terrain.

The shortwave radiation balance in complex terrain is highly variable in space and time, and its contribution to the radiation balance at a snow surface has been taken into account in several models (e.g., Dozier 1980; Munro and Young 1982). Varley et al. (1996) reported an important contribution in the diffuse radiation on slopes.

The variability of the longwave radiation in complex terrain has not been so thoroughly investigated despite the fact that longwave radiation is present day and night and thus considerably influences the energy balance at the surface. Marks and Dozier (1979) presented a model to calculate longwave radiation in mountainous areas, but they neglected the effect of the air between the emitting terrain surface and the receiving snow surface. Olyphant (1986) performed numerical calculations and measurements of longwave radiation in mountainous, snow-covered terrain and pointed out that the anisotropy of the terrain emission (e.g., snow-free areas) and the effects of the air should both be considered.

This study focuses on the relevance of the longwave radiation from terrain in snow-covered alpine environments. Based on radiance calculations with a narrow-band radiation model, the effect of the surrounding topography on the incoming longwave radiation was calculated, including the effects of air between the receiving surface and the emitting topography. An approximate method for the calculation of the longwave irradiance in a terrain model is presented. Some sensitivity studies were performed to detect the conditions under which the longwave radiation from terrain has to be considered for energy balance investigations in snow-covered environments.

Corresponding author address: Dr. Christian Plüss, Institute of Geography, ETH Zurich, Winterthurerstr. 190, 8057 Zurich, Switzerland.
E-mail: pluess@geo.umnw.ethz.ch

TABLE 1. Different cases of atmospheric conditions as they were used in the study. For all cases, the lapse rate was taken as $\Gamma = 5.5$ K km^{-1} up to 4000 m above the surface and the air pressure 1013 hPa at the surface. All other values were taken from the U.S. standard atmosphere for midlatitude winter. The integrated radiance was calculated from wavenumber 0 to 2857 cm^{-1}.

Case	T_a (K) at surface	Cloud conditions
1	263	Clear sky
2	273	Clear sky
3	283	Clear sky
4	273	Low clouds (stratus, stratocumulus; base 0.66 km, top 2.0 km)
5	273	High clouds (altostratus; base 2.4 km, top 3.0 km)

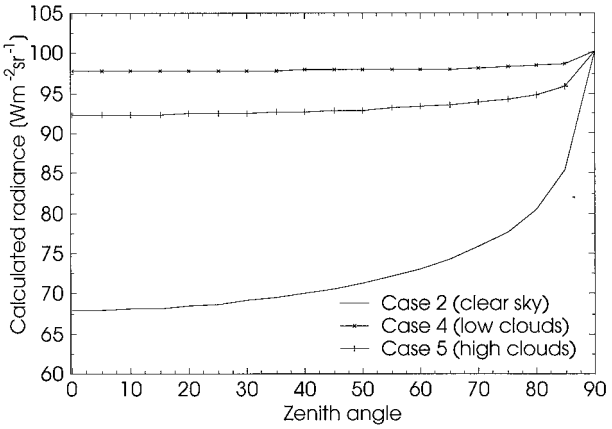

FIG. 1. Variation of the longwave radiance for different cloud conditions calculated with LOWTRAN7. The air temperature near the surface is taken as $T_a = 273$ K. The different model atmospheres are described in Table 1.

2. Longwave radiation from the sky

Longwave irradiance from the sky hemisphere $L_s^{\downarrow}$ may be written as

$$L_s^{\downarrow} = \varepsilon_a \sigma T_a^4, \tag{2}$$

where ε_a is an apparent emissivity of the sky as proposed by Unsworth and Monteith (1975), $\sigma = 5.67 \times 10^{-8}$ W m^{-2} K^{-4} is the Stefan–Boltzmann constant, and T_a is the air temperature near the surface. The apparent emissivity of the sky varies between approximately 0.7 under clear conditions in alpine environments (Kuhn 1987) and close to unity under overcast conditions.

Most incoming longwave radiation reaching the earth's surface is emitted from the lowest layers of the atmosphere; therefore, several simple parameterizations were proposed to estimate the incoming longwave radiation from standard meteorological measurements. Brutsaert (1975) proposed a parameterization for clear conditions based on air temperature T_a and water vapor pressure e_a:

$$L_s^{\downarrow} = 0.642\left(\frac{e_a}{T_a}\right)^{1/7}(\sigma T_a^4). \tag{3}$$

Several variations of (3) were proposed for cloud-covered conditions. Konzelmann et al. (1994) presented a formula for daily mean longwave irradiance from the sky based on measurements under Arctic conditions that also gave good results under alpine conditions (Plüss 1996):

$$L_s^{\downarrow} = \left\{\left[0.23 + 0.483\left(\frac{e_a}{T_a}\right)^{1/8}\right](1 - n^3) + 0.963n^3\right\}\sigma T_a^4, \tag{4}$$

whereby n is the cloud-cover fraction.

For more accurate calculations of the longwave irradiance from the sky a variety of models exist (see Ellingson et al. 1991 for a review). The disadvantages of most of these models are the need for detailed information on the constitution of the atmosphere (usually not available) and the computer time consumption. In this study, longwave radiance was calculated with the widely used narrowband model LOWTRAN7 (Kneyzis et al. 1988). LOWTRAN7 allows for the calculation of the atmospheric transmittance and the background radiance for a given atmospheric path at high spectral resolution (20 cm^{-1}). A description of the most important features of the LOWTRAN model is given in Finger and Kneubühl (1984). Dutton (1993) and Ohmura and Gilgen (1993) compared the measured longwave irradiance at globally diverse locations to LOWTRAN7 calculations and reported a mean underestimation of 5 W m^{-2} under clear conditions.

The LOWTRAN7 sky irradiance was obtained by calculating the integrated radiance between wavenumbers 0 and 2857 cm^{-1} (wavelengths 3.5 μm to infinity) at different zenith angles using several defined atmospheres. The principal model inputs—temperature, air pressure, and humidity—were defined up to 4000 m above the surface. All other values were taken from the U.S. standard atmosphere for midlatitude winter (Table 1). The program was run in thermal radiance mode including multiple scattering.

Figure 1 shows calculated radiance as a function of the zenith angle for three situations under clear and cloudy conditions. Under clear conditions there is an important increase in radiance with the increasing zenith angle, while under cloudy conditions the sky radiance is nearly isotropic.

The irradiance L from any part of the hemisphere may be calculated from the radiance $I_1(\varphi,\theta)$ at the zenith angle θ and the azimuth angle φ by (e.g., Iqbal 1983)

$$L = \int_{\varphi_1}^{\varphi_2}\int_{\theta_1}^{\theta_2} I_1(\varphi, \theta)\sin\theta\cos\theta\, d\varphi\, d\theta. \tag{5}$$

Because the azimuth dependency is negligible for

TABLE 2. Comparison of hemispheric incoming longwave irradiance based on different numbers of zenith angles with LOWTRAN7. The comparison shows numeric integration with Gaussian quadrature using the radiance at different numbers of zenith angles compared with detailed computation with 19 zenith angles based on the Simpson approximation.

Number of angles	Angle θ	Weight for Gaussian quadrature	Case 1 (W m^{-2})	Case 2 (W m^{-2})	Case 3 (W m^{-2})	Case 4 (W m^{-2})	Case 5 (W m^{-2})
1	48.190°	1.0000	183.6	223.2	271.4	307.6	291.5
2	32.333°	0.6361	185.0	225.0	273.8	307.7	292.1
	69.203°	0.3693					
3	24.299°	0.4019	185.1	225.0	274.2	307.7	292.2
	53.805°	0.4585					
	77.740°	0.1397					
4	19.456°	0.2710	185.2	225.1	274.3	307.7	292.2
	43.684°	0.4069					
	65.386°	0.2597					
	81.966°	0.0624					
19	Every 5°		185.2	225.1	274.3	307.6	292.2

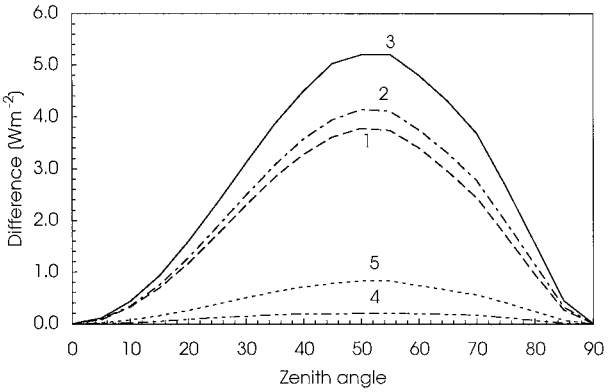

FIG. 2. Difference of incoming longwave irradiance calculated with the Simpson method using angle-dependent radiance minus a calculation based on constant sky radiance. The irradiance is calculated between the horizon and a given zenith angle. The numbers of the curves correspond to the atmospheres as listed in Table 1.

longwave radiation from the sky, the hemispheric irradiance $L^{\downarrow}$ may be obtained by Gaussian quadrature using the calculated radiance at n different zenith angles:

$$L^{\downarrow} = \pi \sum_{i=1}^{n} w_i I_1(\theta_i), \tag{6}$$

whereby w_i is the weight as listed in Table 2 and $I_1(\theta_i)$ is the radiance at the zenith angle θ_i. Table 2 shows that with this method irradiance may be calculated from the radiance at four different zenith angles with the same accuracy as by using Simpson's approximation based on the radiance at 19 different zenith angles. If the radiance at only one zenith angle is used, the accuracy of the hemispheric irradiance is ± 3 W m^{-2} in all these examples.

The assumption of isotropic longwave radiance greatly simplifies the calculation of the sky irradiance. For the calculation of the irradiance in complex terrain, it is, therefore, useful to know if the concept of isotropy is still acceptable for a partly obstructed sky. Figure 2 shows the difference between the irradiance from a sky fraction calculated by (6) using a constant radiance and using Simpson's rule with a zenith-angle-dependent radiance. Despite the large anisotropy of the radiance under clear conditions, the underestimation does not exceed 6 W m^{-2} for all investigated cases with this simplification, independent of the fraction of the sky that is calculated. Under overcast conditions, the error is minimal. Compared to the uncertainty of most currently used longwave radiation instruments, which is 10 W m^{-2} at best (Ohmura and Gilgen 1993), this simplification is considered acceptable for most applications.

3. Longwave radiation from the surrounding topography

In mountainous environments, the radiation from the sky onto a surface is reduced because a portion of the sky is obscured by the surrounding topography. The surface, however, receives additional radiation emitted from the topography as well as from transmission and emission of the air between topography and receiving surface. The longwave irradiance emitted from a snow-covered surface can be calculated based on the Stefan–Boltzmann law:

$$L^{\uparrow} = \varepsilon_s \sigma T_s^4, \tag{7}$$

where T_s is the snow surface temperature and ε_s the emissivity of snow, which is close to unity (Dozier and Warren 1982). In previous studies of the energy balance in complex topography, the longwave radiation from the surrounding terrain was, if included at all, calculated from (7) and multiplied by the thermal view factor (e.g., Marks and Dozier 1979). The effect of the air between the surrounding topography and the surface is usually neglected.

In order to evaluate the importance of the air on the longwave radiation from the surrounding topography, some sensitivity studies were performed. For these sensitivity calculations, the radiance emitted from a surface with temperature T_s, at a given distance and transmitted through a defined atmosphere at different zenith angles, was calculated with LOWTRAN7. Figure 3 shows the variability of the radiance received from an emitting surface with a temperature of $T_s = 273$ K at a zenith angle of $\theta = 90°$ at variable distances through an atmosphere with a given temperature. The distance of the emitting surface has a large influence on the radiance if the surface is close but has only little influence at distances greater than 1 km. In Fig. 4, the calculated radiance from an emitting surface at 1-km distance with variable surface temperature is presented for different zenith angles. The comparison with the sky radiance shows that the zenith angle dependency of the radiance from terrain is very small.

Due to this small sensitivity to emission distance and

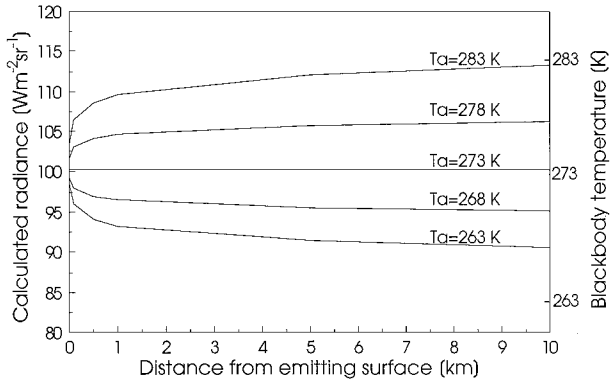

FIG. 3. Calculated radiance received from an emitting surface with temperature $T_s = 273$ K at a zenith angle of 90° and variable distances. The radiance is calculated including the effects of the atmosphere for case 1 (near-surface air temperature $T_a = 263$ K), case 2 ($T_a = 273$ K), and case 3 ($T_a = 283$ K). The corresponding blackbody temperature is indicated for comparison purposes.

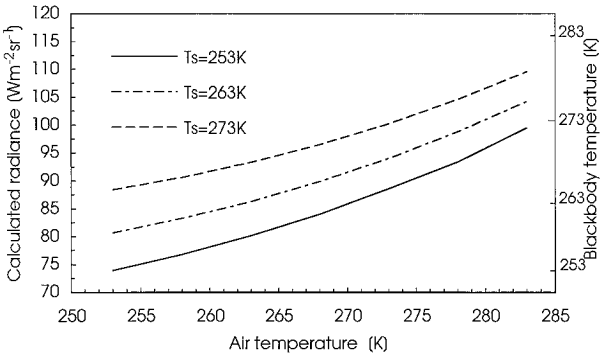

FIG. 5. Variability of the calculated radiance received from an emitting surface at 1-km distance and at 90° zenith angle with changing air temperature for different surface temperatures T_s. The corresponding blackbody temperature is indicated for comparison purposes.

zenith angle, further calculations were performed for a zenith angle of $\theta = 90°$ and for a constant emission distance of 1 km. In Fig. 5, the variability of the calculated longwave radiance is presented as a function of air temperature and surface temperature. If the air temperature is above the temperature of the emitting surface, the calculated radiance is higher than the blackbody radiance of the emitting surface. Under snowmelt conditions, the air temperature is usually above the snow surface temperature (Fig. 6), and thus the calculation of the irradiance, neglecting the effects of air, underestimates the total irradiance.

Based on these findings, a parameterization for the longwave radiance from terrain L_t is proposed:

$$L_t = L_b + aT_a + bT_s, \tag{8}$$

whereby T_a(°C) is the near-surface air temperature, T_s (°C) is the temperature of the emitting snow surface, and a and b are constants determined as $a = 0.77$ W m^{-2} sr^{-1} °C^{-1} and $b = 0.54$ W m^{-2} sr^{-1} °C^{-1}, respectively. The constant L_b is the emitted radiance of a 0°C blackbody that is $L_b = 100.2$ W m^{-2} sr^{-1}.

In order to evaluate the relevance of the radiation from the surrounding topography, the difference of the irradiance between an unobstructed sky and that of a partly obstructed sky was calculated. Figure 7 shows the additional irradiance from the surrounding terrain if the sky is obstructed from topography up to a given elevation angle. On horizontal sites, the elevation angle of the topography exceeds 20° only in very steep mountain valleys; therefore, the additional longwave radiation

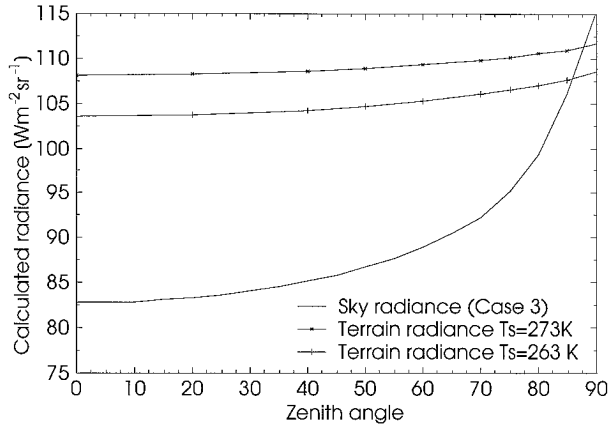

FIG. 4. Radiance received through an atmosphere from an emitting surface at 1-km distance with surface temperature $T_s = 273$ K and $T_s = 263$ K compared to sky radiance. A case 3 atmosphere was taken for all calculations.

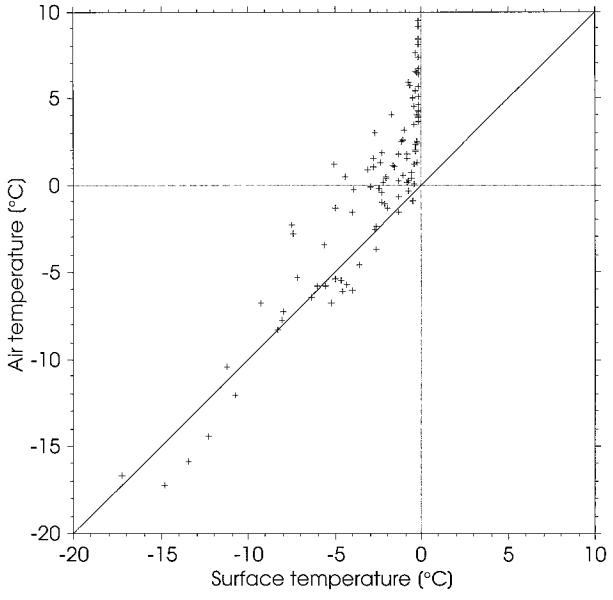

FIG. 6. Air temperature at 2 m above the surface compared to the snow surface temperature obtained from infrared radiation measurements. The measurements were performed on a horizontal site at 2540 m MSL near Davos in the eastern Swiss Alps for the period 20 March–30 June 1993.

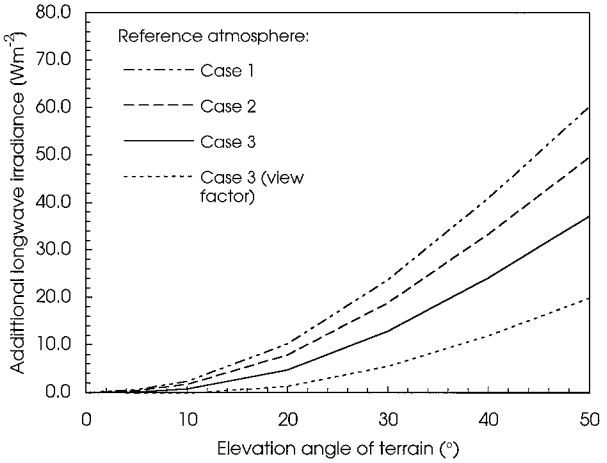

FIG. 7. Additional irradiance onto a surface if the sky is obstructed by topography with surface temperature $T_s = 273$ K up to a given elevation angle. The additional irradiance is calculated as the difference between the irradiance of an unobstructed sky and the irradiance from the surrounding terrain up to the indicated elevation angle. For comparison purposes, the additional irradiance from an emitting surface calculated without the influence of the atmosphere is also shown (283 K, no air).

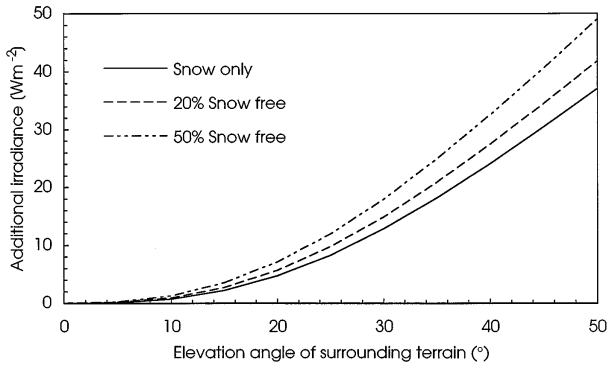

FIG. 8. Additional irradiance from the surrounding topography onto a surface if the sky is obstructed by terrain up to a given elevation angle (as in Fig. 7). Additional longwave irradiance is calculated for a case 3 atmosphere with an emission temperature of 273 K for the snow-covered terrain fraction and 293 K for the snow-free fraction.

from terrain is often negligible for sites on valley floors. However, if the radiation balance on a slope is of interest, a large portion of the hemisphere may be obstructed by the terrain, and the longwave radiation from the surrounding topography may be important and should not be neglected.

During the snowmelt season, alpine snowfields become more and more heterogenous, and the fraction of snow-free areas increases. Olyphant (1986) measured the emission temperature of rock in a snow-covered environment and obtained surface temperatures up to 293 K at 1200 local time. Figure 8 shows the calculated additional longwave irradiance received from completely snow-covered surroundings and from partly snow-free surroundings compared to an unobstructed sky. Due to the effects of the air, the influence of the snow-free areas is relatively small at a distance of 1 km in mostly snow-covered environments.

4. Application to digitized terrain models

For many purposes it is necessary to calculate the energy balance on the grid points of a terrain model. In alpine topography, most surfaces are not horizontal, and for the calculation of the irradiance on such surfaces (4) has to be modified. Kondratyev (1969) gave the basic equations for the calculation of irradiance onto an inclined surface with inclination angle β:

$$L_s^{\downarrow} = \int_0^{2\pi} \int_{H(\varphi)}^{\pi/2} I_{ls}(\theta, \varphi) \cos i \cos H dH \, d\varphi, \qquad (9)$$

$$L_t^{\downarrow} = \int_0^{2\pi} \int_0^{H(\varphi)} I_{lt}(\theta, \varphi) \cos i \cos H dH \, d\varphi, \qquad (10)$$

where $H(\varphi)$ is the elevation angle of the terrain at the azimuth angle φ, I_{ls} is the radiance from the sky, and I_{lt} is the radiance from the surrounding terrain. The angle i, between the vector vertical to the surface and the vector of interest, is given by

$$\cos i = \sin\beta \cos\varphi \cos H + \cos\beta \sin H. \qquad (11)$$

In the previous sections it was shown that the assumption of isotropy for the radiance from the sky and from the surrounding terrain is reasonable in mainly snow-covered environments. Therefore, (9) and (10) may be simplified, assuming I_{ls} and I_{lt} are constant and an algorithm such as that proposed by Funk (1985), for example, may be used to solve these equations. When the surface is very heterogenous and when higher accuracy is needed, it may be necessary to solve (9) and (10) using angle-dependent values for the radiance.

For the calculation of the mean longwave radiance from the surrounding terrain, the snow-surface temperature is needed. Kondo and Yamazaki (1990) proposed a parameterization for its calculation, but the available dataset was not suitable for this method. Therefore, a parameterization for the daily mean surface temperature T_s(°C) is proposed based on standard meteorological variables:

$$T_s = T_a + c_n (n^{1.15} - 0.67) \leq 0°\text{C}, \qquad (12)$$

whereby T_a is daily mean air temperature near the surface, c_n is an empirical constant determined as 7.5°C, and n is the cloud-cover fraction. This parameterization leads to a good estimation of the daily mean snow-surface temperature (Fig. 9).

As an example, the incoming longwave irradiance was calculated for an area in the eastern Swiss Alps on a digitized terrain model using data of an automatic weather station and assuming a constant relative humidity and a lapse rate of 5.5°C km^{-1} (Fig. 10). The sky radiance was calculated for every grid point based on (4), the snow surface temperature based on (12), and

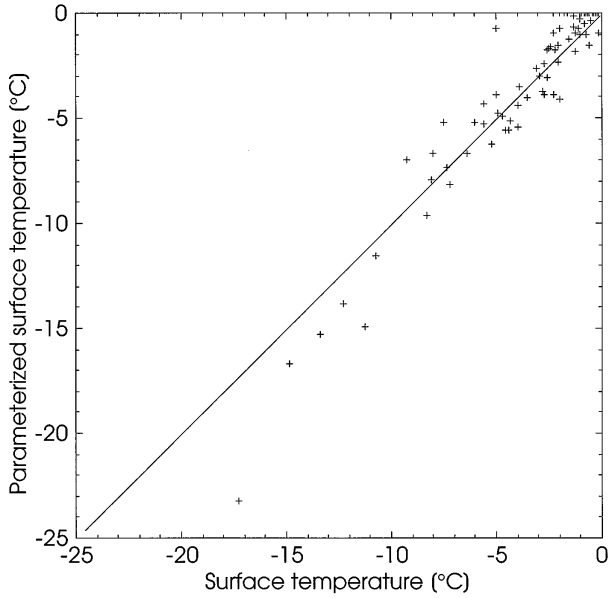

FIG. 9. Daily mean snow surface temperature obtained from infrared radiation measurements (as in Fig. 6) compared to the parameterization proposed in the text [Eq. (12)].

the radiance from the surrounding topography using parameterization (8). Assuming isotropic radiance, the irradiance was obtained by (9) and (10) for every grid point.

The calculated irradiance varies between 160 and 240 W m^{-2} on this clear day, while 162 W m^{-2} was measured on the horizontal site indicated on Fig. 10. The calculated variability is mainly attributed to the topographic influence.

5. Conclusions

For the investigation of longwave irradiance in complex topography, it is necessary to calculate the irradiances from the sky and the surrounding terrain separately. Sensitivity studies based on LOWTRAN7 show that the longwave irradiance received from an obstructed sky depends on the surface temperature of the surrounding terrain and on the air temperature. Assuming isotropic radiance for the sky and terrain radiance, in mostly snow-covered environments the incoming longwave irradiance may be calculated with an error similar to the one currently assumed for radiation instruments. The air between the emitting topography and receiving

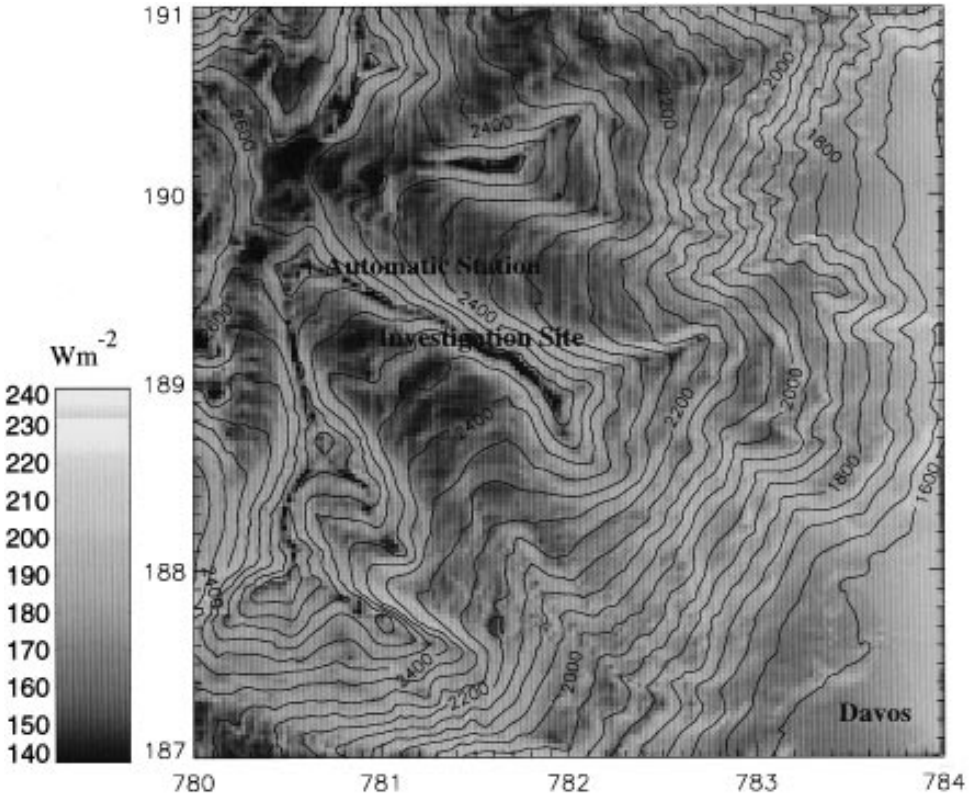

FIG. 10. Calculated longwave incoming radiation for 29 March 1993 on a 4 km × 4 km area in the eastern Swiss Alps near Davos. The input values for the parameterization were obtained from the automatic station indicated in this figure. At the investigation site, 162 W m^{-2} incoming longwave radiation were measured and 159 W m^{-2} calculated. The numbers on the axis indicate the kilometer grid of the Swiss coordinate system.

surface has an effect if the air temperature differs from the temperature of the surrounding terrain surface. In snow-covered environments, where the surface temperature is usually below the air temperature, neglecting the effects of the air leads to an underestimation of the longwave irradiance.

On inclined slopes, the longwave irradiance from the surrounding topography can make an important contribution to the energy balance at the surface, while on horizontal surfaces the effect is usually small compared to the total irradiance from the sky. The proposed parameterization for the calculation of longwave irradiance from terrain includes the effects of air and allows economic calculations of the complete radiation balance in complex, snow-covered terrain.

Acknowledgments. The infrared measurements of the snow surface temperature were provided by the Swiss Federal Institute for Snow and Avalanche Research. Dr. T. Konzelmann made valuable comments on the manuscript.

REFERENCES

Aguado, E., 1985: Radiation balances of melting snow covers at an open site in the central Sierra Nevada, California. *Water Resour. Res.,* **21,** 1649–1654.

Brutsaert, W., 1975: On a derivable formula for long-wave radiation from clear skies. *Water Resour. Res.,* **11,** 742–744.

Dozier, J., 1980: A clear sky spectral solar radiation model for snow covered mountainous terrain. *Water Resour. Res.,* **16,** 709–718.

——, and S. G. Warren, 1982: Effect of viewing angle on the infrared brightness temperature of snow. *Water Resour. Res.,* **18,** 1424–1434.

Dutton, G., 1993: An extended comparison between LOWTRAN7 computed and observed broadband thermal irradiances: Global extreme and intermediate surface conditions. *J. Atmos. Oceanic Technol.,* **10,** 326–336.

Ellingson, R. G., J. Ellis, and S. Fels, 1991: The intercomparison of radiation codes used in climate models: Long-wave results. *J. Geophys. Res.,* **96,** 8929–8953.

Finger, G., and F. Kneubühl, 1984: Spectral thermal infrared emission of the terrestrial atmosphere. *Infrared Millimeter Waves,* **12,** 145–193.

Funk, M., 1985: Räumliche Verteilung der Massenbilanz auf dem Rhonegletscher und ihre Beziehung zu Klimaelementen. *Zürcher Geographische Schriften,* Geographie Institute ETH, 183 pp.

Iqbal, M., 1983: *An Introduction to Solar Radiation.* Academic Press, 390 pp.

Kneizys, F. X., E. P. Shettle, L. W. Abreu, J. H. Chetwynd, G. P. Anderson, W. O. Gallery, J. E. A. Selby, and S. A. Clough, 1988: A Users Guide to LOWTRAN7. Environmental Research Paper 1010, 137 pp. [Available from Air Force Geophysics Laboratory, Hanscom AFB, MA 01731.]

Kondo, J., and T. Yamazaki, 1990: A prediction model for snowmelt, snow surface temperature and freezing depth using a heat balance method. *J. Appl. Meteor.,* **29,** 375–384.

Kondratyev, K., 1969: *Radiation in the Atmosphere.* Academic Press, 912 pp.

Konzelmann, T., R. S. W. van de Wal, W. Greuell, R. Bintanja, E. A. C. Henneken, and A. Abe-Ouchi, 1994: Parameterization of global and longwave incoming radiation for the Greenland ice sheet. *Global Planet. Change,* **9,** 143–164.

Kuhn, M., 1987: Micro-meteorological conditions for snowmelt. *J. Glaciol.,* **33,** 24–26.

Male, D. H., and R. J. Granger, 1981: Snow surface energy exchange. *Water Resour. Res.,* **17,** 609–627.

Marks, D., and J. Dozier, 1979: A clear-sky longwave radiation model for remote alpine areas. *Arch. Meteor. Geophys. Bioclimatol.,* **27,** 159–178.

Munro, D. S., and G. J. Young, 1982: An operational net shortwave radiation model for glacier basins. *Water Resour. Res.,* **18,** 220–230.

Ohmura, A., 1982: Climate and energy balance on the arctic tundra. *J. Climatol.,* **2,** 65–84.

——, and H. Gilgen, 1993: Re-evaluation of the global energy balance. *Interactions between Climate Subsystems: The Legacy of Hann, Geophys. Monogr.,* No. 75, IUGG, 93–110.

Olyphant, G., 1986: Longwave radiation in mountainous areas and its influence on the energy balance of alpine snowfields. *Water Resour. Res.,* **22,** 62–66.

Plüss, C., 1996: The energy balance over the Alpine snow cover—Point measurements and areal distribution. Ph.D. dissertation, Swiss Federal Institute of Technology, Zürich, Switzerland, 116 pp. [Available from Geographie ETH, Winterthurerstr. 190, 8057 Zurich, Switzerland.]

Unsworth, M., and L. Monteith, 1975: Longwave radiation at the ground: I Angular distribution of incoming radiation. *Quart. J. Roy. Meteor. Soc.,* **101,** 13–24.

Varley, M. J., K. J. Beven, and H. R. Oliver, 1996: Modelling solar radiation in steeply sloping terrain. *J. Climatol.,* **16,** 93–104.